



Additively manufactured porous titanium alloy scaffolds for orthopaedics: An effect of process parameters on porosity

Palash Mondal¹ , Hrittik Dey², Sreetama Paul², Shamik Sarkar², Apurba Das³, Amit Karmakar¹

¹Department of Mechanical Engineering, Jadavpur University, Kolkata, 700032, India

²Department of Mechanical Engineering, Techno Engineering College Banipur, Habra, 743233, India

³Department of Aerospace Engineering and Applied Mechanics, Indian Institute of Engineering Science and Technology, Shibpur, 711103, Howrah, India

Email: palashmondal.ju@gmail.com

Article History

Received: 2 March 2022

Accepted: 21 April 2022

Keywords:

Additive manufacturing;
selective laser melting;
porous scaffolds;
3D printing

Abstract

Titanium alloys have been widely used as metallic materials for additive manufacturing, especially selective laser melting in recent decades because of its great corrosion resistance, excellent mechanical properties and biocompatibility. Solid titanium alloys have higher compressive strength and elastic modulus than natural human bones and to get similar results that of human bones, solid titanium alloys are replaced by porous titanium alloys to fulfil the orthopaedic demands in biomedical applications. In this study two different types of Ti scaffolds (Grid and Vinties, each of two, total number of four) were designed using 3D CAD software with 65% porosity and fabricated through SLM process. The process parameters, employed in the work like laser power, hatch distancing, scanning speed, and layer thickness are the most effective factors that affect the porosity of the SLM-fabricated samples. The results demonstrate that when the porosity percentage increases, the energy density, scanning speed, and hatch distancing rise, but the laser power drops. This study primarily focuses on to determine porosity of the fabricated scaffolds by Archimedes principle and optimizing the process parameters. Finally, compressive test is carried out on the scaffolds in an INSTRON machine of maximum ± 25 kN load capacity. The result shows better capability to manufacture with minimum error in porosity percentage and good potential for orthopedic applications as metallic implants.

1. Introduction

Ti-6Al-4V is a most general form of titanium alloy which is commonly employed in orthopaedic and dental applications. Its superior performance and wide variety of applications in the military and commercial industries, Ti-6Al-4V is referred to as "space metal" or "ocean metal" (Leyens and Peters). With widespread use of the titanium alloy in bio-

medical domains in recent decades, it is becoming more common to produce Ti-6Al-4V alloy devices with complicated structures (Ju et al. Bartolomeu et al.). Traditional manufacturing process is unable to match the demands of complicated shapes like internal channels, space progressively shifting surfaces, and ultrathin walls.

Metal AM methods, particularly SLM process,

have been produced to eliminate the bottleneck. SLM melts the powders in layer upon layer to produce a strong metallurgical link between them without the use of any additional instruments. It has the potential to construct purely dense and complicated structures. However, there are a number of issues to make a completely dense element by SLM process (Nicola and Schiavone). As a result, increasing the density of SLM fabricated samples has been a major priority for many researchers. Furthermore, a unique microstructure has been seen during the SLM process as a result of the severe non-equilibrium condition. Li et al. optimized the parameters of Ti-6Al-4V scaffolds fabricated by SLM via Taguchi method (Li et al.) looked at the effect of layer thickness on performance (Shi et al.) presented a revised model that helps to understand the connection between mechanical properties and input process parameters (Tiwari et al.) investigated heat transfer simulation model based on process parameters (junfeng and zhengying) discussed the effect of laser power, layer thickness, scanning speed, and hatch distancing on microstructures (Khorasani et al.) were studied the effect of input process parameters of Al-Si-10Mg manufactured by SLM (Butler et al.). Jin et al. investigated the control of porosity content in Co-Cr-Mo fabricated by SLM (Joguet et al.). studied the potential of microstructure of Ti-6Al-4V alloy manufactured by SLM at different scan speeds (Pei et al.) investigated microstructure of selectively laser melted Ti-6Al-4V alloy at different energy densities (Nan and Jin). It has been observed that input process parameters are the primary elements that influence the microstructure of SLM fabricated samples, and process optimization of Ti-6Al-4V fabrication is still needed. The goal of the present work is to look at the influence of process parameters (laser power, hatch distancing, and scanning speed) on porosity and relative density of Ti-6Al-4V made by SLM, and to find an optimal range of process parameters.

2. Material Selection and Methods

Gas atomized Ti-6Al-4V powders, supplied by Supplied by EOS GmbH (Germany), were employed in this work. The morphology of Ti-6Al-4V powder was investigated optical microscope Olympus BX41 or GX51 (EOS, Finland) as shown in Fig. 1 and a nearly spherical shape with smooth surface was

observed. In this work, two different type scaffolds (Grid and Vinties, each of two, total 2x2=4) of 15 mm cube and 65% porosity were designed in 3D CAD software and manufactured by SLM process (shown in Fig. 2). Then the scaffolds were heat treated through 800°C for 120 minutes. To retain an environment with a low oxygen concentration throughout construction, initially the building chamber is emptied then the chamber is filled with an inert gas (argon). A specific density of 4.41 g/cm³ and relative density 100% (Approx.) for Ti64 was used.

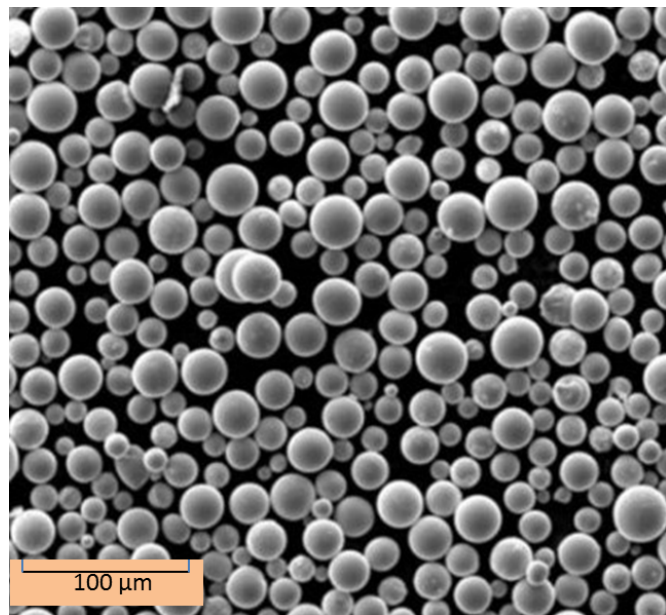


FIGURE 1. SEM morphology of Ti-6Al-4V powders

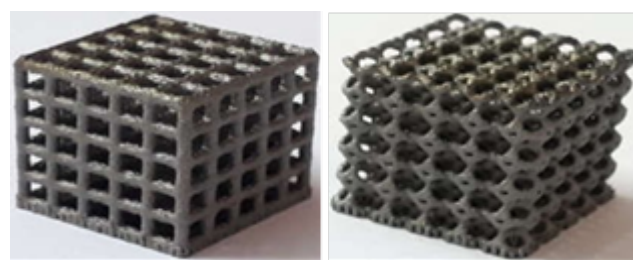


FIGURE 2. Porous Ti-6Al-4V scaffolds by SLM

The SLM technique depends on some selected process input parameters like energy density, scanning speed, laser power, hatch distancing and layer thickness and the relationship between them can be expressed as:

$$E_d = P_l / (v_s h_t) \dots 1$$

Where E_d = energy density, P_l = laser power, v_s = scan speed, h_d = hatch distancing and t = layer thickness.

The porosity percentage (P) depends on the process parameters, energy density (E_d), scanning speed (v), laser power (P_l) and hatch distancing (h) and the relationship between them can be expressed as:

$$P = f(E_d v_s h^2) / p_1 \quad \dots 2$$

3. Result and Discussion

3.1. Optimisation of process parameters during SLM

The porosity of produced samples are influenced by input process parameters like scanning speed, laser power, hatch spacing, and layer thickness during the SLM process. The scaffolds were made using a SLM machine (Model: EOSINT M280-400W) with the input process parameters for TI-6AL-4V materials. An optimization analysis is necessary to set the suitable process parameters for getting the desired density during manufacturing by SLM. The optimized process parameters are shown in Table 1.

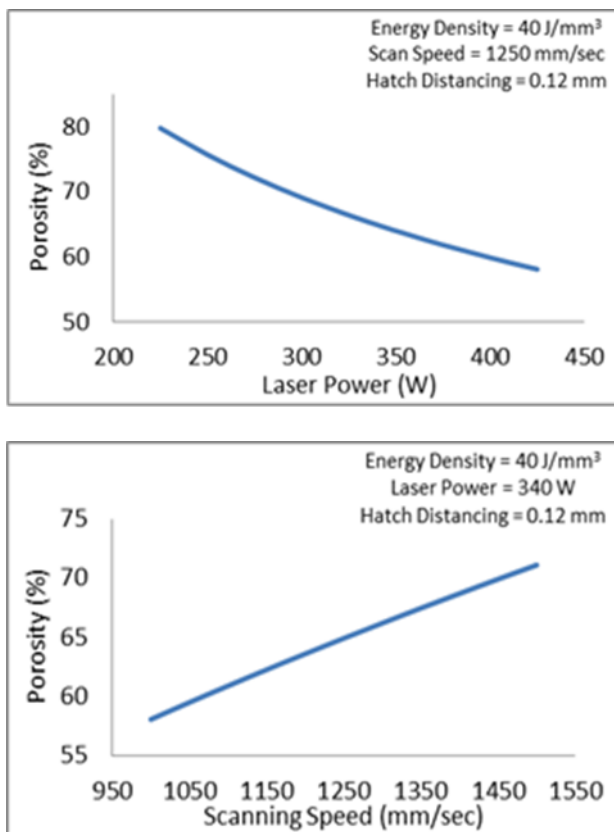


FIGURE 3. Effect of process parameters on porosity during SLM

From Fig. 3, it is observed that with increase in laser power, porosity % decreases and on the other hand porosity % increases with scanning speed.

3.2. Porosity measurement of porous scaffolds

The porosity of the manufactured samples is measured through density principle. In a minutely graded testing cylinder, each sample is immersed in water. The quantity of displaced water gives the theoretical volume of the porous scaffold as shown in Fig. 4. By subtracting the actual volume of the sample without porosity from the theoretical volume of the scaffold with porosity, the porosity data is determined (shown in Fig. 5). The grid type of samples has the lowest percentage of porosity inaccuracy than vinties type, as seen in Fig. 6.

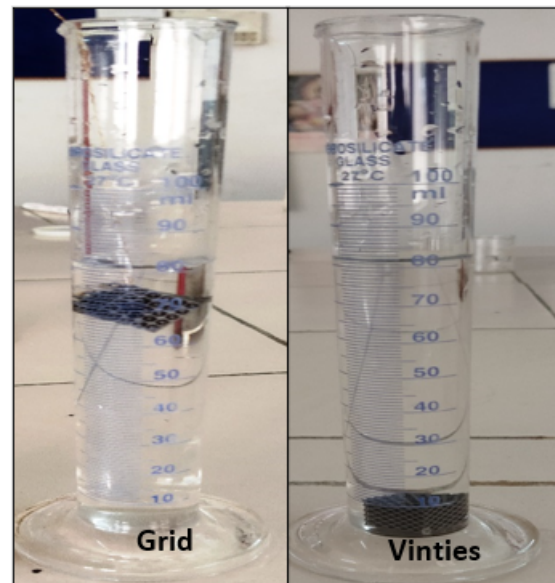


FIGURE 4. Porosity measurement of scaffolds by measuring cylinder

The porosity of the scaffolds can be calculated as:

$$P = (1 - V_p/V_d) \times 100\% \quad \dots 3$$

Where P = porosity, V_p = solid volume of the porous sample and V_d = overall volume of the densified sample. The measured porosity of each samples are listed in Table 2.

From Fig. 5, it is observed that the grid type of samples has the lowest percentage error in porosity that of vinties type. With a low variation of porosity difference between the modeled and fabricated samples, the grid type sample might provide better similarities.

3.3. Compression test

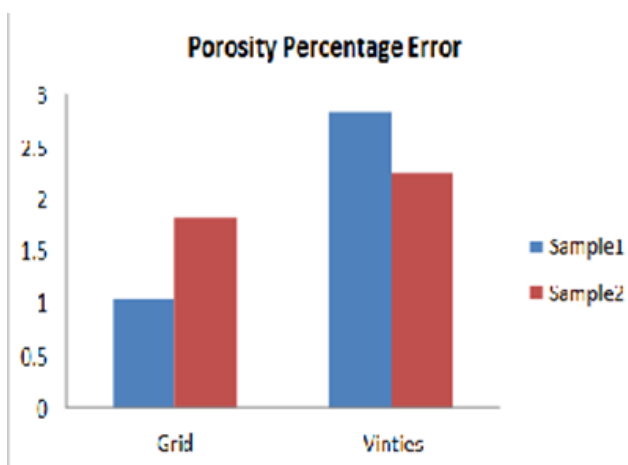
To measure the mechanical properties, all of the samples were compressed uniaxially in an INSTRON machine (maximum ± 25 kN load capacity). A TAB attached to the machine is used to set

TABLE 1. Input process parameters used in SLM process for Ti-6Al-4V.

Parameters	Value
Type of Laser	Ytterbium Fibre Laser
Scan Speed	1250 mm/Sec
Particle Diameter	80 μm
Hatch Distance	0.12 mm
Laser Power	340 W
Density	4.41g/cm ³
Thickness of Layer	0.06 mm
Scan Angle of Rotation	67 ⁰
Environment Maintained	Inert
Scan Path	"X" & Rotational

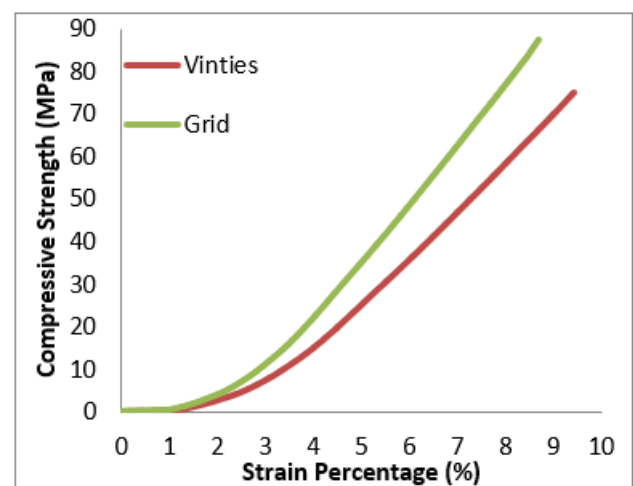
TABLE 2. Measured porosity of the fabricated samples

Sample Type	Designed porosity	Actual porosity	
		Sample 1	Sample 2
Grid	65%	63.97%	63.18%
Vinties	65%	62.16%	62.76%

**FIGURE 5.** Error in porosity percentage of fabricated scaffolds by SLM

up the machine's initial settings as well as to control it. The change in load applied and deformation responses are recorded for each sample in a computer which was pre-connected to the INSTRON machine during the test. Under normal atmospheric circumstances (28⁰C and 65 % RH), all scaffolds are compressed at a crosshead movement rate of 0.02 mm/sec. Finally, using the recorded data, the stress-strain curve is plotted (shown in Fig. 6).

The compressive modulus of elasticity is determined by the slope drawn on the stress-strain curve. Fig. 6 shows the values of modulus of elasticity and compressive strength of grid and vinties samples obtained from INSTRON are 10.56 GPa & 8.87

**FIGURE 6.** Compressive stress vs staincurve for the porous Ti-6Al-4V scaffolds

GPa and 87.2 MPa & 75 MPa respectively. When can be seen from the results, the grid sample is slightly tough at first due to its form, but as the wire distorts under load, it becomes soft and the strain rises. The fabricated scaffolds have a promising elastic modulus ($E = 4 - 30$ GPa (Becerikli and Mustafa)) that is equivalent to native cortical bones. Table 3 demonstrates that it has a greater compressive strength than bone (compressive strength ranges from 0.45 to 25.8 MPa (Martens et al.)). The stress-shielding effect is reduced as a result of the enhanced compressive strength, but the implant's

TABLE 3. Comparison of mechanical properties between fabricated porous Ti-6Al-4V scaffolds and natural cortical bones

Material	Scaffold Type	Mechanical Properties	
		Elastic Modulus (GPa)	Compressive Strength (MPa)
Ti-6Al-4V	Grid	10.56	87.2
	Vinties	8.87	75
Natural bone	-	4 - 30	0.45 – 25.8

lifespan is extended.

4. Conclusion

In this work two different type of porous Ti-6Al-4V scaffolds were designed using 3D CAD software of 15mm cube with 65% porosity and manufactured by SLM process. Titanium alloys, have excellent mechanical properties, biocompatibility, corrosion resistance and low cost, are the most useful metallic biomaterials in the field of orthopaedic and dental implants. To upgrade mechanical property, the porous scaffolds were heat treated at 800°C for 120 minutes in the presence of inert atmosphere, and at last cooled at room temperature in a furnace. The process parameters are optimized as: 340 W laser power, 1250 mm/sec scanning speed, 0.12 mm powder layer thickness and 0.06 mm hatch spacing. AM-fabricated scaffolds have marginally lower porosities than designed scaffolds, resulting in relative elastic modulus and mechanical strength deviations. The grid type of sample has the lowest error percentage in porosity than vinties type. The elastic modulus of manufactured samples is very similar to the human bones, but compressive strength is higher than human bones, which may aid to lessen the effect of stress-shielding and extend the implant's lifespan and can be successfully applied to biomedical fields.

ORCID iDs

Palash Mondal  <https://orcid.org/0000-0001-8417-8938>

References

Bartolomeu, F., et al. "Implant surface design for improved implant stability – A study on Ti6Al4V dense and cellular structures produced by Selective Laser Melting". *Tribology International* 129 (2019): 272–282. [10.1016/j.triboint.2018.08.012](https://doi.org/10.1016/j.triboint.2018.08.012).

Becerikli and Mustafa. "P2000-A high-nitrogen austenitic steel for application in bone surgery".

Plos one 14 (2019). [10.1371/journal.pone.0214384](https://doi.org/10.1371/journal.pone.0214384).

Butler, C., et al. "Effects of processing parameters and heat treatment on thermal conductivity of additively manufactured AlSi10Mg by selective laser melting". *Materials Characterization* 173 (2021): 110945–110945. [10.1016/j.matchar.2021.110945](https://doi.org/10.1016/j.matchar.2021.110945).

Joguet, David, et al. "Porosity content control of CoCrMo and titanium parts by Taguchi method applied to selective laser melting process parameter". *Rapid Prototyping Journal* 22.1 (2016): 20–30. [10.1108/rpj-09-2013-0092](https://doi.org/10.1108/rpj-09-2013-0092).

Ju, Jiang, et al. "Effect of heat treatment on microstructure and tribological behavior of Ti-6Al-4V alloys fabricated by selective laser melting". *Tribology International* 159 (2021): 106996–106996. [10.1016/j.triboint.2021.106996](https://doi.org/10.1016/j.triboint.2021.106996).

junfeng, Li and Wei zhengying. "Process Optimization and Microstructure Characterization of Ti6Al4V Manufactured by Selective Laser Melting". *IOP Conference Series: Materials Science and Engineering* 269.1 (2017): 012026–012026. [10.1088/1757-899x/269/1/012026](https://doi.org/10.1088/1757-899x/269/1/012026).

Khorasani, Amir Mahyar, et al. "A survey on mechanisms and critical parameters on solidification of selective laser melting during fabrication of Ti-6Al-4V prosthetic acetabular cup". *Materials & Design* 103 (2016): 348–355. [10.1016/j.matdes.2016.04.074](https://doi.org/10.1016/j.matdes.2016.04.074).

Leyens, Christoph and Manfred Peters. "Titanium and titanium alloys: fundamentals and applications". *John Wiley & Sons* (2003). [10.1002/3527602119](https://doi.org/10.1002/3527602119).

Li, Zhonghua, et al. "Optimising the process parameters of selective laser melting for the fabrication of Ti6Al4V alloy". *Rapid Prototyping Journal* 24.1 (2018): 150–159. [10.1108/rpj-03-2016-0045](https://doi.org/10.1108/rpj-03-2016-0045).

Martens, M., et al. “The mechanical characteristics of cancellous bone at the upper femoral region”. *Journal of Biomechanics* 16.12 (1983): 971–983. [10.1016/0021-9290\(83\)90098-2](https://doi.org/10.1016/0021-9290(83)90098-2).

Nan and Jin. “Effects of heat treatment on microstructure and mechanical properties of selective laser melted Ti-6Al-4V lattice materials”. *International Journal of Mechanical Sciences* 190 (2021). [10.1155/2021/6646588](https://doi.org/10.1155/2021/6646588).

Nicola and Schiavone. “Effect of 3D Printing Temperature Profile on Polymer Materials Behavior”. *3D Printing and Additive Manufacturing* (2020). [10.1089/3dp.2020.0175](https://doi.org/10.1089/3dp.2020.0175).

Pei, Wei, et al. “Numerical simulation and parametric analysis of selective laser melting process of AlSi10Mg powder”. *Applied Physics A* 123.8 (2017): 1–15. [10.1007/s00339-017-1143-7](https://doi.org/10.1007/s00339-017-1143-7).

Shi, Xuezhi, et al. “Effect of high layer thickness on surface quality and defect behavior of Ti-6Al-4V fabricated by selective laser melting”. *Optics & Laser Technology* 132 (2020): 106471–106471. [10.1016/j.optlastec.2020.106471](https://doi.org/10.1016/j.optlastec.2020.106471).

Tiwari, Jitendar Kumar, et al. “Investigation of porosity, microstructure and mechanical proper-

ties of additively manufactured graphene reinforced AlSi10Mg composite”. *Additive Manufacturing* 33 (2020): 101095–101095. [10.1016/j.addma.2020.101095](https://doi.org/10.1016/j.addma.2020.101095).



© Palash Mondal et al. 2022 Open Access.

This article is distributed under the terms of the Creative Commons Attribution 4.0 International License (<http://creativecommons.org/licenses/by/4.0/>), which permits unrestricted use, distribution, and reproduction in any medium, provided you give appropriate credit to the original author(s) and the source, provide a link to the Creative Commons license, and indicate if changes were made.

Embargo period: The article has no embargo period.

To cite this Article: Mondal, Palash, Hrittik Dey, Sreetama Paul, Shamik Sarkar, Apurba Das, and Amit Karmakar. “**Additively manufactured porous titanium alloy scaffolds for orthopaedics: An effect of process parameters on porosity.**” *International Research Journal on Advanced Science Hub* 04.04 April (2022): 88–93. <http://dx.doi.org/10.47392/irjash.2022.023>